34th Annual International Conference of the IEEE EMBS
San Diego, California USA, 28 August - 1 September, 2012

Potential of MREIT Conductivity Imaging to Detect Breast Cancer: Experimental and Numerical Simulation Studies

Saurav Z. K. Sajib, Hyung Joong Kim, Young Tae Kim, Woo Chul Jeong, Tong In Oh, *Member, IEEE,* and Eung Je Woo, *Senior Member, IEEE*

***Abstract*— The conductivity values of cancerous tissues in the breast are significantly higher than those of surrounding normal tissues. Breast imaging using MREIT (Magnetic Resonance Electrical Impedance Tomography) may provide a new noninvasive way of detecting breast cancer in its early stage. In breast MREIT, the conductivity image quality highly depends on the amount of injected currents assuming a certain signal-to-noise ratio (SNR) of an MRI scanner. The injected current should not produce any significant adverse effect especially on the nerve conduction system of the heart and still distinguish a small cancerous anomaly inside the breast. In this paper, we present results of experimental and numerical simulation studies of breast MREIT. From breast phantom experiments, we evaluated practical amounts of noise in measured magnetic flux density data. We built a realistic three-dimensional model of the human breast connected to a simplified model of the chest including the heart. We performed numerical simulations of various scenarios in breast MREIT including different amplitudes of injected currents and predicted SNRs of MR images related with imaging parameters. Simulation results are promising to show that we may detect a cancerous anomaly in the breast while restricting the maximal current density inside the heart below a level of nerve excitation.**

I. Introduction

Early diagnosis is the key to increase the survival rate from the breast cancer. There have been active researches on imaging the breast based on the fact that cancerous tissues in the breast have much higher conductivity values than those of normal breast tissues [1,2]. Several electrical impedance imaging methods and experimental studies have shown their pros and cons in detecting a cancerous anomaly in the breast from conductivity images [3-7]. However, all of these impedance imaging methods have not yet reached the stage of routine clinical uses primarily due to their limitations in spatial resolution, accuracy and reproducibility.

Magnetic resonance electrical impedance tomography (MREIT) is a new bio-imaging modality to produce high-resolution conductivity images using an MRI scanner [8]. It is based on the current-injection MRI technique where the MRI scanner is used to obtain the images of internal magnetic flux density (B_z) distributions induced by externally injected currents [9,10]. Numerous conductivity image reconstruction methods have been suggested to produce conductivity images with a pixel size of a few millimeters [11]. Kim *et al* [12] presented MREIT human leg imaging results and suggested numerous clinical applications. MREIT may potentially be useful for the diagnosis of breast cancer if we can restrict the amount of injected currents not to produce adverse effects especially on the nerve conduction system of the heart.

In this paper, we perform a feasibility study of breast MREIT incorporating the latest technical developments in MREIT. We will first describe experimental studies using a breast phantom to evaluate noise levels in measured magnetic flux density data from a clinical MRI scanner. We will then present three-dimensional numerical simulation studies of a realistic breast model to find whether one can distinguish a small anomaly in the breast from reconstructed conductivity images. Connecting the breast model to a simplified chest model including the heart, we will also check the amount of current density in the heart produced by externally injected currents through electrodes on the surface of the breast.

II. Methods

A. Breast Phantom Imaging Experiment

We built an acrylic phantom of the thorax (30×14×15 cm^3) and breast (11 cm in diameter). After filling the phantom with saline having conductivity of 0.12 S/m, two different biological tissues of porcine muscle and chicken breast were positioned in the phantom (Fig. 1a). Their conductivity values were 0.64 and 0.60 S/m, respectively. We attached four carbon-hydrogel electrodes around the breast area of the phantom and chose the electrode configuration in figure 1(b) for two current injections (I_1, I_2).

We placed the phantom inside the bore of the 3T MRI scanner (Siemens Medical Solutions, Erlangen, Germany) with a multi-channel breast coil. Using a custom-designed MREIT current source, we injected the current varying the amplitude from 3 to 0.5 mA with the total pulse width of 30 ms. We used the multi-echo ICNE pulse sequence [13] with TR/TE = 800/20 ms, FOV = 180×180 mm^2, slice thickness = 4 mm, number of averaging = 8, matrix size = 128×128, and number of slices = 7.

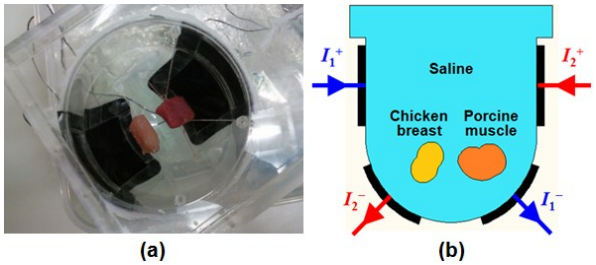

Fig. 1. (a) Top-view of breast phantom with two different biological tissues and (b) current injection method.

Authers are with the Department of Biomedical Engineering, Kyung Hee University, Gyeonggi-do 446-701 KOREA (phone: +82-31-201-2538; fax: +82-31-201-2378; e-mail: ejwoo@ khu.ac.kr).

B. Noise Estimation

Since we extract B_z data from acquired MR phase images, they are contaminated by noise, of which amount is the primary limiting factor in detecting an anomaly from a reconstructed conductivity image. We can express the noise standard deviation **s** in measured B_z data as

$$\mathbf{s} = \frac{1}{\sqrt{2}\gamma \mathbf{T}_c \mathbf{Y}_M} \tag{1}$$

where $\gamma = 26.75\times10^7$rad/T•s is the gyromagnetic ratio of hydrogen, T_c is the total current injection time and Y_M is the signal-to-noise ratio (SNR) of the MR magnitude image [14]. Using (1), we can estimate the noise level in measured B_z data from phantom imaging experiments. Here, we note that the MR magnitude image SNR Y_M is influenced by numerous imaging parameters as well as tissue properties such as T1 and T2 values. Since we need to estimate the noise standard deviation in measured B_z data from the human breast, we consider the following conversion formula:

$$\mathbf{s} = \frac{\mathbf{s}_0}{\frac{\mathbf{T}_c}{\mathbf{T}_{c0}}\frac{\Delta_x}{\Delta_{x0}}\frac{\Delta_y}{\Delta_{y0}}\frac{\Delta_z}{\Delta_{z0}}\frac{1-\mathbf{e}^{-\frac{\mathbf{TR}}{\mathbf{T1}}}}{1-\mathbf{e}^{-\frac{\mathbf{TR}_0}{\mathbf{T1}_0}}}\frac{\mathbf{e}^{-\frac{\mathbf{TE}}{\mathbf{T2}}}}{\mathbf{e}^{-\frac{\mathbf{TE}_0}{\mathbf{T2}_0}}}\sqrt{\frac{\mathbf{N}\mathbf{N}_x\mathbf{N}_y\mathbf{N}_z\Delta\mathbf{t}}{\mathbf{N}_0\mathbf{N}_{x0}\mathbf{N}_{y0}\mathbf{N}_{z0}\Delta\mathbf{t}_0}}} \tag{2}$$

where Δ_x, Δ_y, Δ_z are pixel sizes, N is the number of averaging, N_x, N_y, N_z are numbers of pixels and Δt is the dwell time. Note that the subscript 0 indicates the values for the case where the noise standard deviation $\mathbf{s_0}$ is evaluated from a certain imaging experiment.

C. Numerical Simulation

We built a three-dimensional model of the breast connected with simplified chest region including the ellipsoid shape heart as shown in figure 2(a). In-order to produce more uniform current distribution inside breast we attached two large pair of electrodes. The discretized model consists of 319,753 tetrahedral and 44,263 triangular elements. In this simulation, quadratic interpolation function with 2,985,532 degrees of freedom was used. Table 1 summarizes conductivity values of the different tissues used in the numerical simulation, described in Gabriel *et al* [15].

Table 1. Conductivity values of different tissues used in numerical simulations. The conductivity of the cancerous anomaly was assumed to be five times larger than that of the glandular tissue. For the chest and heart regions, we used average conductivity values of different tissues included in the regions.

Region	Glandular tissue	Subcutaneous fat	Chest	Heart
Conductivity [S/m]	0.0226	0.0196	0.2194	0.3480

Using the MREIT simulator [16], we generate two independent current voltage u_j and current densities $\mathbf{J}_j$ and estimate magnetic flux densities $B_{z,j}$ for j = 1, 2 using Bio-Savert law. In the simulated $B_{z,j}$ data, we added Gaussian noise of proper standard deviation values computed by using (2). For conductivity image reconstructions, we used the harmonic B_z algorithm [17, 18] implemented in CoReHA (conductivity reconstructor using harmonic algorithms) [19].

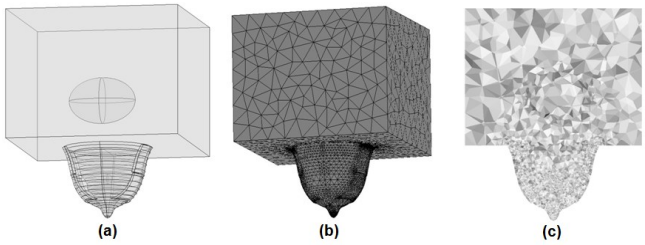

Fig. 2. (a) Three-dimensional model, (b) mesh and (c) quality of mesh element.

III. Results

A. Breast Phantom Images and Noise Estimation

Figure 3(a), (b) and (c) are reconstructed conductivity images of the breast phantom using 3, 1 and 0.7 mA injection currents, respectively. Using the noise estimation method described in Sadleir *et al* [14], we evaluated the SNR Y_M of the acquired MR magnitude images and the noise level $\boldsymbol{s}$ in the B_z images and summarized the values in table 2.

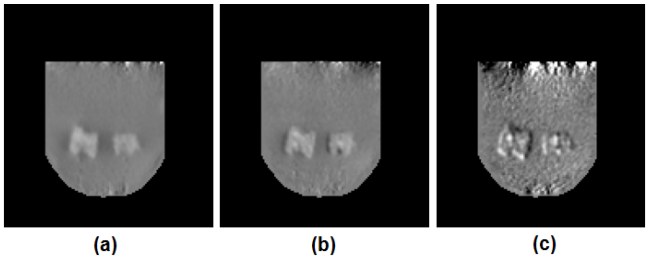

Fig. 3. Reconstructed conductivity images of the breast phantom using different amounts of injected currents: (a) 3, (b) 1 and (c) 0.7 mA.

Table 2. MR magnitude image SNR Y_M and noise standard deviation $\boldsymbol{s}_0$ in B_z images from the breast phantom experiment.

Region	Background	Chicken breast	Porcine muscle
SNR, Y_M	1566	290	332
Noise standard deviation, $\boldsymbol{s}_0$ [nT]	0.0578	0.3118	0.2724

B. Simulation Results

Figure 4(a), (b) and (c) are plots of the computed voltage u_1, magnitude of current density $|\mathbf{J}_1|$ and magnetic flux density $B_{z,1}$ for the injected current I_1 without any anomaly. We plotted differences of Δu_1, $\Delta|\mathbf{J}1|$ and $\Delta B_{z,1}$ when the three anomalies with 10, 5 and 2.5 mm diameters was included. We can see that the anomaly perturbed the distributions of u_1, $\mathbf{J}_1$ and $B_{z,1}$ and note that the values of $\Delta B_{z,1}$ in the anomaly region must be greater than the noise level in measured $B_{z,1}$ data. We found similar results for the second injection current I_2.

Figure 5 plots true and reconstructed conductivity images of the three anomalies by using the computed noise-free data of $B_{z,1}$ and $B_{z,2}$ using the harmonic B_z algorithm [17,18]. Without noise, the MREIT imaging method can differentiate

an anomaly as long as its size is bigger than the pixel size of 1.4 mm.

Figure 6 shows reconstructed conductivity images of the three anomalies with 10, 5 and 2.5 mm diameters depending on different numbers of NEX and current amplitudes. The conductivity images clearly demonstrate the advantage of larger injection current amplitude and a larger number of averaging at the expense of an increased scan time. Since the total scan time may not be a critical limiting factor in breast imaging, we suggest increasing the number of averaging and reducing the current amplitude below 1 mA.

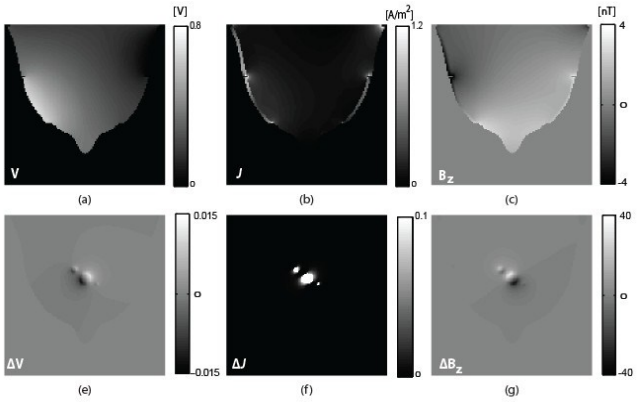

Fig. 4. Plots for noise-free (a) u_1, (b) $|\mathbf{J}_1|$ and (c) $B_{z,1}$. (d), (e) and (f) are plots of Δu_1, $\Delta|\mathbf{J}_1|$ and $\Delta B_{z,1}$ which are differences between the cases without and with anomaly of 10, 5 and 2.5 mm diameter.

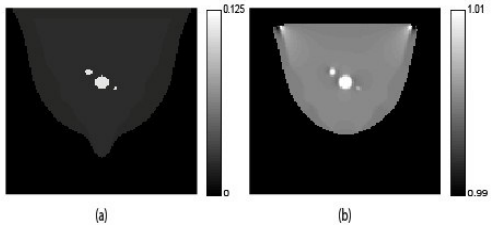

Fig. 5. Plots of conductivity (a) true and (b) reconstructed, for the three different anomalies (10, 5 and 2.5 mm diameters, respectively).

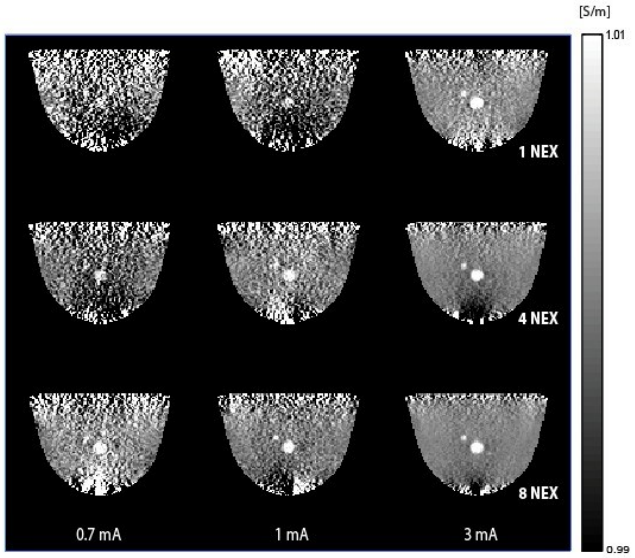

Fig. 6. Reconstructed conductivity images of the three anomalies with 10, 5 and 2.5 mm diameters using different numbers of averaging N and current amplitude.

C. Comparison of ΔB_z with Noise Level

Figure 7 represents quantitative analysis of the average ΔB_z and noise levels of B_z depending on the different conductivity contrast and size of anomaly. The conductivity images with a pixel size of 3 or 4 mm may visualize an anomaly with 50% conductivity contrast and 5 mm diameter using 1 mA injection currents. Considering that conductivity values of cancerous tissues in the breast have much higher than 50% contrast compared with surrounding normal tissues, it is highly probable to distinguish an anomaly with a smaller than 5 mm diameter using 1 mA injection currents.

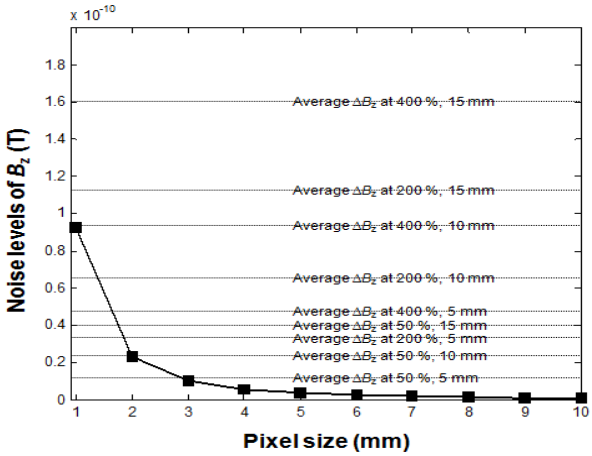

Fig. 7. Comparisons of the average ΔB_z with the noise level in B_z. The noise level was computed with T_c = 30 ms, N = 8 and Δz = 4 mm. We changed the conductivity contrast of the anomaly as 50, 200 and 400% and the diameter as 5, 10 and 15 mm. The background conductivity is 0.0226 S/m.

D. Current Density Estimation in the Heart Region

We examined the magnitude of the internal current density distribution induced by 3 mA injection current, which is the largest amount in our simulations. The maximum current density inside the heart region was below 0.14 A/m^2. We estimated the threshold of nerve stimulation as 1.2 A/m^2 at a distance of 1 mm from the nerve. Since the estimated maximum current density inside the heart region is well below this threshold, we speculate that externally injected currents of 3 mA or lower will not stimulate the nerve conduction system of the heart.

IV. Discussion

Compared with the previous breast phantom results [20], the images in figure 6 show the importance of the electrode size and configuration. Two current injections through large and flexible electrodes covering most of the breast surface can produce more uniform current density distributions inside the breast. Since the magnetic measured flux density B_z at a position is strongly influenced by the current density there, uniform current density distributions inside the breast region are advantageous in detecting an anomaly which may exist anywhere in the breast. The adopted electrode configuration using two pairs of electrodes also exhibited its limitation since they should have produced small current densities around the base and apex regions of the breast. This, in turn, should have produced small values of induced B_z data there. For a same

amount of noise in measured B_z data throughout the entire breast region, these two local areas of the base and apex are more vulnerable to the noise. We may consider adding electrodes at the back of the chest and also on the apex of the breast to improve the overall image quality.

Plots in figure 7 tell that conductivity images with a pixel size of 3 or 4 mm may visualize an anomaly with 50% conductivity contrast and 5 mm diameter using 1 mA injection currents. Considering that conductivity values of cancerous tissues in the breast have much higher than 50% contrast compared with surrounding normal tissues, it is highly probable to distinguish an anomaly with a smaller than 5 mm diameter using 1 mA injection currents.

Though we did not show other plots of numerous different experimental scenarios, we may easily scale up and down the plots in figure 7 for different conditions. We will design breast MREIT experiments of animals and human subjects based on the analysis method presented in this paper. Carefully designed experimental protocols will minimize the expensive trial-and-error type learning process during such experimental MREIT imaging studies.

V. Conclusion

We found that breast cancer detection using MREIT is feasible. Simulation results indicate that a cancerous anomaly with less than 5 mm diameter can be detected by injecting less than 1 mA currents while restricting the maximal current density inside the heart region below a level of nerve excitation. As we decrease the current amplitude, the size of a detectable anomaly will increase. Based on the findings presented in this paper, we suggest breast MREIT imaging experiments using four large flexible uniform current density electrodes covering the breast surface as much as possible. Advanced breast MR imaging methods including multi-channel high-sensitivity breast RF coils should be employed to minimize the noise level in measured magnetic flux density data. In MREIT, the performance of the adopted MRI scanner is essential to improve the quality of reconstructed conductivity images. Using a high performance clinical 3T MRI scanner, we plan to conduct animal and human imaging experiments to further investigate the clinical usefulness of the proposed method.

Acknowledgment

This work was supported by the National Research Foundation of Korea (NRF) grant funded by the Korea government (MEST) (No. 20100018275).

References

[1] A. J. Surowiec, S. S. Stuchly, J. R. Barr, A. Swarup, "Dielectric properties of breast carcinoma and the surrounding tissues," *IEEE Trans. Biomed. Eng*., vol. 35, pp. 257-263, 1988.

[2] J. E. Silva, J. P. Marques, J. Jossinet, "Classification of breast tissue by electrical impedance spectroscopy," *Med. Biol. Eng. Comput*., vol. 38, pp. 26-30, 2000.

[3] V. Cherepenin, A. Karpov, A. Korjenevsky, V. Kornienko, Y. Kultiasov, M. Ochapkin, O. Trochanova, J. Meister, "Three-dimensional EIT imaging of breast tissues: system design and clinical testing," *IEEE Trans. Med. Imag*., vol. 21, pp. 662-667, 2002.

[4] T. E. Kerner, K. D. Paulsen, A. Hartov, S. K. Soho, S. P. Poplack, "Electrical impedance spectroscopy of the breast: clinical imaging results in 26 subjects," *IEEE Trans. Med. Imag*., vol. 21, pp. 638-645, 2002.

[5] M. Assenheimer, O. Laver-Moskovitz, D. Malonek, D. Manor, U. Nahliel, R. Nitzan, A. Saad, "The T-Scan technology: electrical impedance as a diagnostic tool for breast cancer detection," *Physiol. Meas*., vol. 22, pp. 1-8, 2001.

[6] B. Scholz, "Towards virtual electrical breast biopsy: space-frequency MUSIC for transadmittance data," *IEEE Trans. Med. Imag*., vol. 21, pp. 588-595, 2002.

[7] J. K. Seo, O. Kwon, H. Ammari, E. J. Woo, "Mathematical framework and anomaly estimation algorithm for breast cancer detection: electrical impedance technique using TS2000 configuration," *IEEE Trans. Biomed. Eng*., vol. 51, pp. 1998-2004, 2004.

[8] E. J. Woo, J. K. Seo, "Magnetic resonance electrical impedance tomography (MREIT) for high-resolution conductivity imaging," *Physiol. Meas*., vol. 29, pp. R1-R26, 2008.

[9] M. L. G. Joy, G. C. Scott, R. M. Henkelman, "*In vivo* detection of applied electric currents by magnetic resonance imaging," *Magn. Reson. Imag*., vol. 7, pp. 89-94, 1989.

[10] G. C. Scott, M. L. G. Joy, R. L. Armstrong, R. M. Henkelman, "Measurement of nonuniform current density by magnetic resonance," *IEEE Trans. Med. Imag*., vol. 10, pp. 362-374, 1991.

[11] J. K. Seo, E. J. Woo, "Magnetic resonance electrical impedance tomography (MREIT)," *SIAM Rev.*, vol. 52, pp. 40-68, 2011.

[12] H. J. Kim, Y. T. Kim, A. S. Minhas, W. C. Jeong, E. J. Woo, J. K. Seo, O. J. Kwon, "*In vivo* highresolution conductivity imaging of the human leg using MREIT: the first human experiment," *IEEE Trans. Med. Imag*., vol. 28, pp. 1681-1687, 2009.

[13] A. S. Minhas, W. C. Jeong, Y. T. Kim, Y. Q. Han, H. J. Kim, E. J. Woo, "Experimental performance evaluation of multi-echo ICNE pulse sequence in magnetic resonance electrical impedance tomography," *Magn. Reson. Med.*, vol. 66(4), pp. 957-965, 2011.

[14] R. Sadleir, S. Grant, S. U. Zhang, B. I. Lee, H. C. Pyo, S. H. Oh, C. Park, E. J. Woo, S. Y. Lee, O. Kwon, J. K. Seo, "Noise analysis in MREIT at 3 and 11 Tesla field strength," *Physiol. Meas*., vol. 26, pp. 875-884, 2005.

[15] S. Gabriel, R. W. Lau, C. Gabriel, "The dielectric properties of biological tissues: II. Measurements in the frequency range 10 Hz to 20 GHz," *Phys. Med. Biol*., vol. 41, pp. 2251-2269, 1996.

[16] A. S. Minhas, H. H. Kim, Z. J. Meng, Y. T. Kim, H. J. Kim, E. J. Woo, "Three-dimensional MREIT simulator of static bioelectromagnetism and MRI," *Biomed. Eng. Lett.,* vol. 1, pp. 129-136, 2011.

[17] S. H. Oh, B. I. Lee, E. J. Woo, S. Y. Lee, M. H. Cho, O. Kwon, J. K. Seo, "Conductivity andcurrent density image reconstruction using harmonic *Bz* algorithm in magnetic resonance electrical impedance tomography," *Phys. Med. Biol*., vol. 48, pp. 3101-3116, 2003.

[18] J. K. Seo, J. R. Yoon, E. J. Woo, O. Kwon, "Reconstruction of conductivity and current density images using only one component of magnetic field measurements," *IEEE Trans. Biomed. Eng*., vol. 50, pp. 1121-1124, 2003.

[19] K. Jeon, C. O. Lee, H. J. Kim, E. J. Woo, J. K. Seo, "CoReHA: conductivity reconstructor using harmonic algorithms for magnetic resonance electrical impedance tomography (MREIT)," *J. Biomed. Eng. Res*., vol. 30, pp. 279-287, 2009.

[20] B. I. Lee, S. H. Oh, T. S. Kim, E. J. Woo, S. Y. Lee, O. Kwon, J. K. Seo, "Basic setup for breast conductivity imaging using magnetic resonance electrical impedance tomography," *Phys. Med. Biol*., vol. 51, pp. 443-455, 2006.